International Journal of Research in Geography (IJRG)
Volume 1, Issue 1, June 2015, PP 38-51
www.arcjournals.org

Identification and Visualization of Vegetation Encroachments along Power Line Corridors using LiDAR

KURINSKY, Brian

Harris Corporation
Advanced Geospatial Services
Melbourne, Florida
USA

HUNG, Ming-Chih

Department of Humanities and Social Sciences
Northwest Missouri State University, Maryville
Missouri. USA
mhung@nwmissouri.edu

Abstract: *Electric power has effectively become the life blood of modern society. To follow the metaphor, it seems just as sensible that diagnostic methods that avert a stroke or heart attack in humans need to be applied to preventing power outages and blackouts and their devastating impact on human lives and economic activity. Vegetation such as trees adds beauty and value to the landscape but still proves to be one of the leading causes of power outages and blackouts in the United States. For this reason, management of vegetation along power line corridors is of the utmost importance to utility companies. At its core, this involves identification and removal of vegetation deemed dangerously close to conductors and other hardware. This article focuses on the dangerous vegetation identification effort. Many utility companies still cling to legacy methods of surveying power line corridors to identify encroaching vegetation to be removed, such as ground field surveys. These methods were constrained by the lack of technology for a time, but the emergence of new technology offers much more effective and efficient methods.*

One such technology, Light Detection and Ranging (LiDAR), was used to identify vegetation encroachments along several power line corridors located in a residential/commercial section of Callahan, FL, United States; just outside the city of Jacksonville. A semi-automatic process was used to generate LiDAR-derived conductor line vectors, on which a buffer algorithm was run. This resulted in LiDAR points being reclassified which were within a dangerous distance of the conductor vectors. These vegetation encroachment points were aggregated into polygon regions of vegetation to be removed, and the polygons were viewed over an imagery background in several applications.

Keywords: *Power line corridor; vegetation management; LiDAR; blackout; electricity*

1. INTRODUCTION

1.1. Threats to Precious Electricity

The North American electricity system is one of the greatest achievements in engineering over the past century. This infrastructure represents more than $1 trillion (U.S.) in asset value, has over 200,000 miles of transmission lines, 950,000 megawatts of power generation capability, and nearly 3,500 utility organizations serving well over 100 million customers and 283 million people. Modern society has come to depend greatly on reliable electricity as an essential resource for national security; health and welfare; communications; finance; transportation; food and water supply; heating, cooling, and lighting; computers and electronics; commercial enterprise; and certainly entertainment and leisure (U.S.-Canada Power System Outage Task Force, 2004).To put it succinctly, nearly all aspects of modern life are supported by electricity. It is no wondered why delivering electric power reliably is of the utmost importance to utility companies. Not to mention if meters are not running, no profit is being made. Still, even in such an industrious country as the U.S., it is estimated that economic losses due to power outages range from $50 billion to $100 billion every year (Ituen et *al*., 2008). This problem requires attention.

Understanding how power outages and blackouts occur is the first step in moving toward preventing them. According to the Edison Electric Institute (EEI) 62% of all power outages in the U.S. have been weather/tree-related (EEI, 2013). EEI has lumped trees and weather into one category because it is more likely for weather to cause a tree to interfere with a power line rather than a tree interfering on its own. Trees affect power lines in two major ways:(1) Mechanical tear-down and (2) Electrical short circuits or arcs causing over current faults. Mechanical tear-down refers to any action that breaks mechanical supporting insulators, rips conductors from poles, or breaks and drops conductors. This

would be any object, usually a tree, which falls into a conductor and tears it down. Arcs and short circuits occur when a tree bridges the gap between two or more conductors or causes two or more conductors to come into contact with one another. An example would be a branch falling over two parallel energized phase conductors built on horizontal cross arms. Frequently, a combination of both tear-down and short circuit events occur. In fact, either type of event can occur first, leading to the second. For example, lines torn down by trees (mechanical tear-down) can cause conductors to arc when they hit the ground, creating an electrical short circuit. Conversely, an electrical short circuit can burn conductors in two, and cause them to fall to the ground (Texas Engineering Experiment Station, 2011).

A glaring example of a tree-related power failure incident is the Northeast Blackout of 2003, which affected an estimated 55 million people in the U.S. and Canada. During an August afternoon, when power usage and ambient air temperature were very high, several transmission line conductors sagged toward the ground enough to contact trees beneath them. This caused a cascading blackout due to the second type of tree interference mentioned above. After investigation by the U.S.-Canada Power System Outage Task force, it was determined that nothing was wrong with the transmission conductors, but rather trees in certain areas were not maintained correctly and were allowed to grow too tall (U.S.-Canada Power System Outage Task Force, 2004). It was also determined that the interfering trees had passed an inspection only months prior to the blackout, so something was apparently wrong with the inspection process (Ituen et *al*., 2008).

1.2. Legacy Inspection Methods Vs. LiDAR

Historically, manual inspection methods have been used by a majority of utility companies to manage rights-of-way (ROW) vegetation, including the company that conducted the inspection on the failed lines which caused the Northeast Blackout of 2003 (Young, 2011). These mostly include foot and/or vehicle patrols and aerial patrols by helicopter while using various tools and techniques for measuring distances between vegetation and power lines (Mills et al., 2010). These methods are labor intensive and many times too subjective.

It has been argued that LiDAR provides a better solution than other approaches with regard to obtaining accurate 3D positional information of features along power line corridors. Zhang et al. (2008) maintained that commonly used tools such as digital video cameras, infrared cameras, and telescopes lack high spatial positioning precision, and multi-source data from these methods are processed separately. They argued that a LiDAR system with an integrated digital camera for ortho photos can overcome these disadvantages due to the nature of the laser pulses it emits. The pulses are reflected from ground objects and return to the sensor, where the distance to objects and strength of reflectance are measured. These provided a means by which to differentiate objects such as vegetation, buildings, power lines, poles, etc. Chen et al. (2006) noted another disadvantage to traditionally used power line survey and design methods such as aerial Photogrammetric. They also agreed that photogrammetric methods do not allow penetration of the tree canopy to the ground surface, and vegetation height information could not be obtained. In an experiment conducted in May of 2006 by the Central Southern China Electric Power Design Institute, LiDAR was proven to perform well enough to serve as a potential approach to power line design (Chen et al., 2006). Yang and Xu (2009) took full advantage of the utility of LiDAR data in China by using it to identify "risky" objects along power line corridors, automatically measure clearance distances between vegetation and conductors, measure distances between conductors, use 3D visualization to manage power lines, and perform topography change detection. You et al. (2013) calculated inclination and displacement of power towers, wire bending, line crossover, and vegetation encroachment which the authors called "space check."

Two meaningful quantitative studies that were conducted with regard to the accuracy of LiDAR compared to legacy power line corridor dangerous vegetation identification techniques are as follows: The first was conducted by American Electric Power (AEP) in Ohio. In an attempt to better its processes, a Light Detection and Ranging mission was flown over 2,500 miles of transmission lines to identify any immediate or potential vegetative threats that may have been missed by the company's helicopter surveillance team, which typically flew along all transmission lines at least annually (Jobes et al., 2008).The comparison of these two techniques revealed 247 additional critical events where vegetation or tree growth represented a serious threat to power lines, more than AEP's existing methods had found. Figure 1 shows one such event.

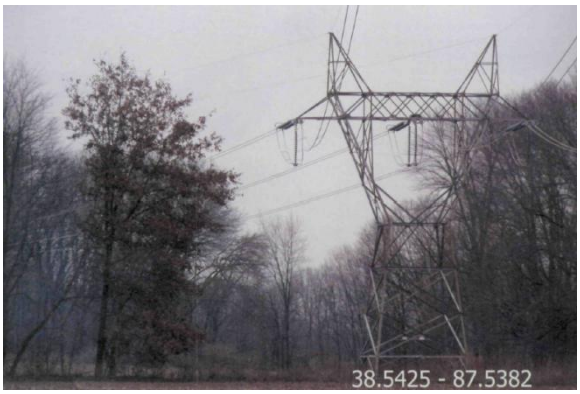

Figure1. *A tree missed by AEP's aerial survey but identified with LiDAR.*

Prior to the employment of LiDAR technology, it was never possible for AEP to be 100% sure that all vegetation had been removed or that it had been removed well enough to eliminate the immediate threat. For the first time ever, LiDAR allowed the AEP team to measure the performance of a vegetation management vendor and ensure that threats were mitigated swiftly (Jobes et al., 2008).

In the second study Bonneville Power Administration (BPA), a federal nonprofit agency based in the Pacific Northwest and part of the Department of Energy, five power line corridor vegetation inspection techniques were compared in order to critically evaluate vegetation management programs in place in the utility industry (Narolski, 2010). Inspection techniques included (1) ground inspection by BPA personnel, (2) helicopter survey by BPA personnel, (3) helicopter survey by natural resource specialists, (4) ground inspection by contracted private firm, and (5) LiDAR remote sensing (figure 2).

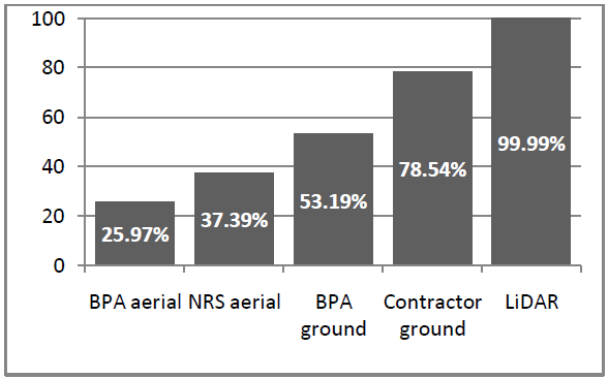

Figure2. *Accuracy comparison of BPA's inspection techniques*

As determined by BPA, LiDAR outperformed all other field inspection techniques by locating the most clearance violations. This was true even after accounting for an approximate 12% rate of false positives found in verifying LiDAR reports in the field. These false positives were objects other than vegetation such as transmission line hardware, light poles, abandoned wood poles, and birds (Narolski, 2010). LiDAR stood out in this study because of the number offalse negatives found in more subjective, human-based inspection methods. While the LiDAR approach located some false clearance issues, other methods missed real clearance issues.

1.3. Research Objective

Few studies like the two mentioned above, which actually quantify the accuracy of LiDAR compared to legacy methods of vegetation encroachment detection, have been documented via the literature or otherwise. The studies that did this have proven LiDAR is far superior to visual ground and visual aerial inspections. The objective of this research is to identify encroaching vegetation along power line corridor and visualize them in various media for various work environments.

2. STUDY AREA AND DATA SOURCES

2.1. Study Area

The study area covers approximately 11 linear kilometers of 69 kilovolt distribution power line corridors in a residential/commercial section of Callahan, Florida, United States, just outside the city

of Jacksonville (figure 3). These power lines are characteristic of those many would see while driving around town, perhaps to and from work or the grocery store (figure 4).Distribution lines, sometimes referred to as 'feeder lines' in the utility industry, distribute electricity from substations to businesses and residential neighborhoods. Figure 4 shows that it is immediately apparent there is vegetation growing in close proximity to power lines in the study area, but the distances between the two are not yet known.

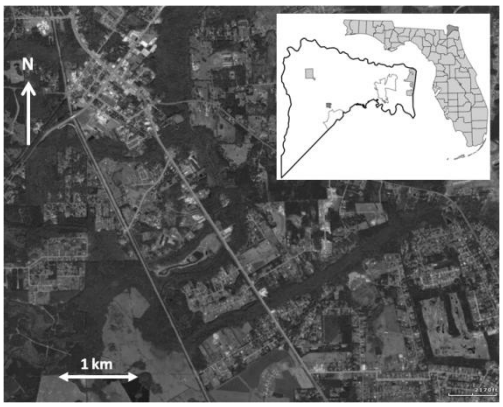

Figure3. *Power line corridors in the study area*

Figure4. *Power lines in the study area*

2.2. Data Sources

The two datasets used in this study consist of a LiDAR point cloud and aerial image orthomosaic, both collected along the corridors noted in figure 3. The two datasets were collected in tandem from two sensors mounted to a Cessna 207 single engine aircraft.

2.2.1.LiDAR

Table 1 shows metadata for the LiDAR dataset used in this study. Figure 5 shows a sample of the LiDAR dataset, figure 6 shows the entire LiDAR collection, and figure 7 shows a sample of the LiDAR as classified by the vendor.

Table1. *LiDAR Meta data*

Data Format	LAS (.las)
Sensor	Leica Geosystems ALS60
Sensor Mode	Linear
Coordinate System	NAD 1983 State Plane Florida East – FIPS 0901
Collection Date	5/30/2012
Point Density	35 points/meter2
Vertical/Horizontal Accuracy	15 centimeters

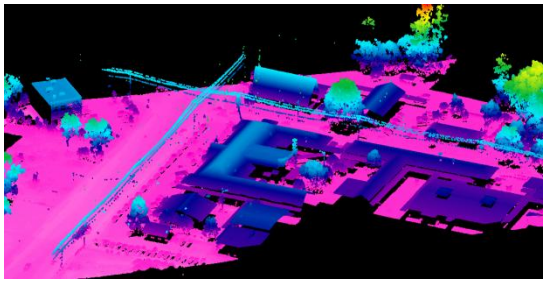

Figure5. *A sample of the LiDAR dataset over the study area*

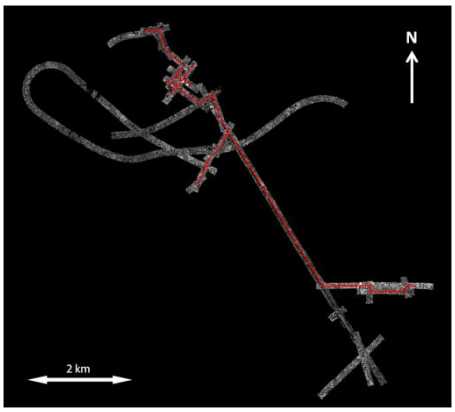

Figure6. *The entire LiDAR dataset with power line vectors overlaid*

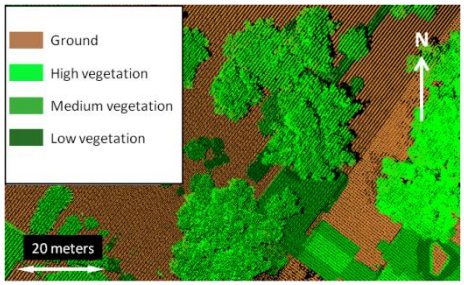

Figure7. *A sample of the LiDAR dataset as classified by the vendor*

The LiDAR dataset was processed by the vendor after collection to include formatting to LAS and a quick classification. The classes used were ground (class 2), low vegetation (class 3), medium vegetation (class 4), and high vegetation (class 5) from the American Society for Photogrammetry and Remote Sensing LAS 1.4 specification. The building class was not used due to time constraints for processing. In figure 5 the conductors can clearly be seen (light blue), which is the result of the relatively high average point density of 35 points per square meter. This makes the dataset ideal for power line analysis.

2.2.2. Aerial Imagery

Table2 shows metadata for the aerial image orthomosaic used in this study. Figure 8 shows a sample of the orthomosaic.

The aerial imagery originated as a series of separate images collected over the power line corridors in the study area at the same time as the LiDAR data. The data vendor processed the images to output an orthomosaic as a single enhanced compressed wavelet file. The high spatial resolution of the image allows the narrow conductors to be seen as a result.

3. METHODOLOGY

Figure 9 shows the workflow used in this study. The process starts with a LiDAR point cloud and ends with vegetation encroachment polygons and conductor vectors in shape file and KML formats.

3.1. Identification of Power Poles and Conductors

First, the support poles holding up the conductors were defined in the form of vertical line vector data in 3D space using specialized software. This was based on the LiDAR data, where the top and bottom of each pole were selected in the point cloud, and then a vertical line was automatically drawn between the top and bottom points (figure 10). This process was repeated in 3D space along each corridor in the study area until all support poles in the LiDAR data had associated vertical vector lines.

Table2. *Metadata for the aerial imagery*

Image Format	Enhanced Compressed Wavelet (ECW), (.ecw)
Sensor	Leica RCD-105 Medium Format Digital Aerial Camera
Spectral Sensitivity	True color RGB
Spatial Resolution	.0762meters per pixel
Collection Date	5/30/2012
Coordinate System	NAD 1983 StatePlaneFloridaEast - FIPS0901 - Feet (2236)

Figure8. *A sample of the aerial image orthomosaic*

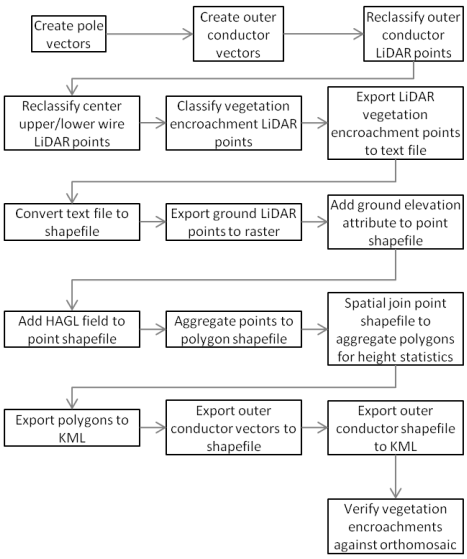

Figure9. *The workflow used in this study*

Next, the LiDAR data points that represent conductors in the point cloud were used to extract vector lines which represent the conductors. For this effort each conductor span between support pole vectors was visited and a semi-automatic approach was used. For each span between poles, four or more seed points were selected from the LiDAR data which were used by the software to construct each conductor line vector. Based on the seed points for each conductor span, the software constructed each vector with a "best fit" algorithm. This was repeated for each conductor in the study area, resulting in line vectors for all conductors in the LiDAR dataset (figure 11).

At this point a collection of vector data has been created, which includes all conductors and support poles in the study area. The next steps deal with reclassifying points in the cloud that represent the conductors from the high vegetation class (class 5) to the power line class (class 14). This is necessary in order to avoid having these points become classified as vegetation encroachments in later steps. The reclassification of the conductor LiDAR points was accomplished using a 3D buffer of 0.5 meters around all conductor vectors. When run, the buffer algorithm changed the class of all points within 0.5 meters of the conductor vectors from high vegetation to power line. A buffer distance of 0.5 meters was chosen in order to affect only conductor points without erroneously changing any non-conductor points such as vegetation or other features.

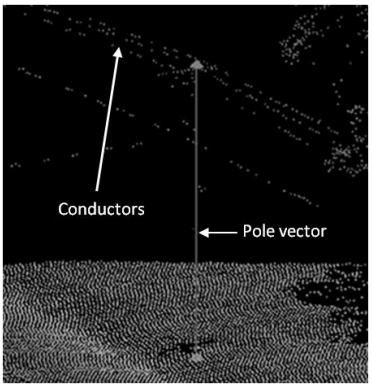

Figure10. *A vertical line vector pole*

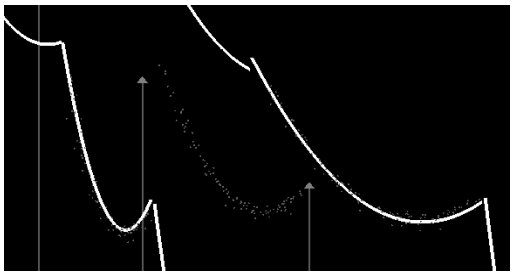

Figure11. *Conductor vectors and LiDAR points*

Only the outer wires are conductors, so these are the only LiDAR points in the point cloud put in the power line class so far. Referring back to figure 10, there are three wires on the top and one wire below those. The top center wire is a ground wire, and the bottom wire carries cable television and/or telephone signals. These wires will need to be reclassified from high vegetation to power line as well, however. Since line vector data is not needed for the ground and cable television wires, it will not be extracted; therefore reclassification of these points cannot be accomplished by a buffer. The LiDAR points representing these wires were reclassified manually by viewing them in a 2D profile, selecting groups of them and applying a classification command (figure 12). This was repeated for all remaining wire points in the study area LiDAR dataset (figure 13).

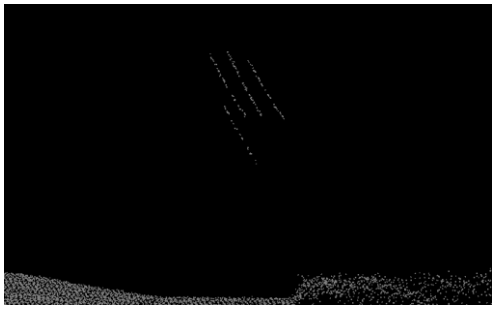

Figure12. *Manually reclassified ground and cable TV/telephone wires in 2D profile view.*

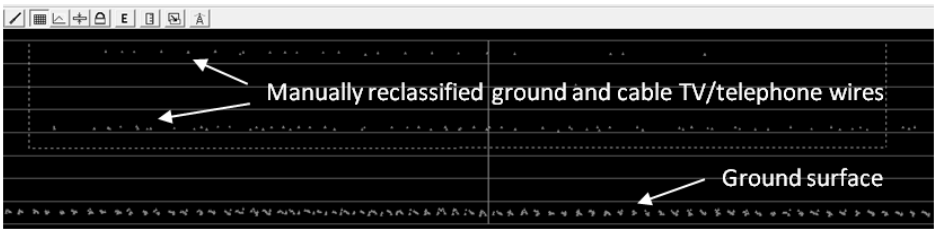

Figure13. *A sample of all wires in the study area dataset classified as power line.*

3.2. Identification of Encroaching Vegetation

Vegetation encroachment analysis can take place now that all the prerequisite steps have been performed. First, the decision was made as to what constitutes a vegetation encroachment. For this study an encroachment was established as any LiDAR vegetation point falling within a 1.5 meter 3D buffer around each set of conductor span line vectors. This buffer differs from the one used to reclassify the conductors. Instead of the tube-like buffer surrounding the conductor vectors, a U-shaped 'clear sky' buffer was used to identify vegetation encroachments (figure 14).

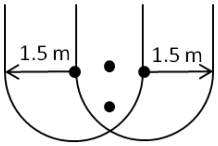

Figure14. *Clear sky buffer*

It is called a clear sky buffer because the top of it in 3D space is open, and the sides infinitely reach upward toward the sky. The effect of a wall on either side of each conductor is created. When applied, this buffer will identify any vegetation points within 1.5 meters of both conductors, no matter how tall they are. This is especially important for any vegetation that may be dangerously hanging over the power lines and could fall into them.

Inputs for the buffer operation were made, which include buffer type, buffer radius, existing classes to be reclassified, and what class the points will ultimately be assigned as a result of the reclassification. Class 13 was originally called Wire Guard in the LAS 1.4 specification, but for this study was renamed to ROI (Region of Interest) for convenience, since it is next to the Power Line class (class 14). The buffer type was set to clear sky (vice regular like the conductor point classification) and the buffer radius was set to 1.5 meters, as discussed. The classes to be reclassified were set to 3, 4, and 5, which are the vegetation classes that include everything except for the wires (class 14) and the ground surface (class 2). Classes 3, 4, and 5 were set to be reclassified to the new class, ROI (class 13). The buffer operation was then run, resulting in any points in classes 3, 4, or 5 that fell within the clear sky buffer to be reclassified to class 13, ROI (figures 15 and 16).

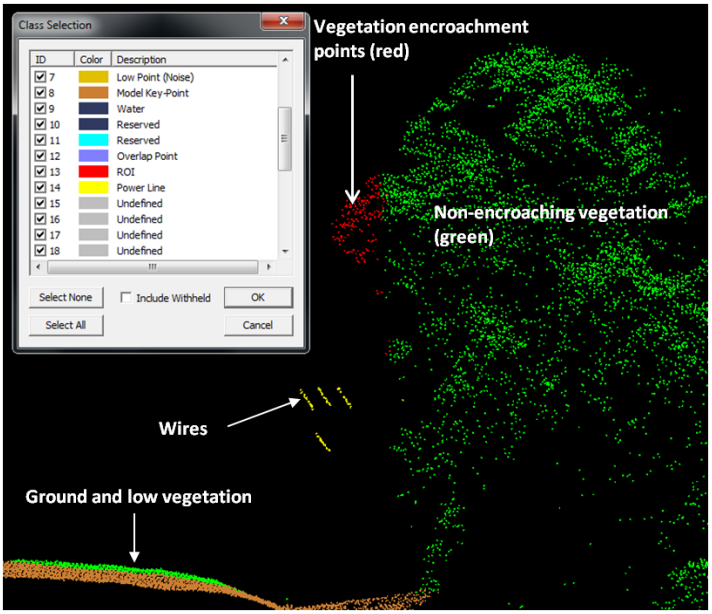

Figure15. *A sample of the results of the clear sky buffer operation in 3D space*

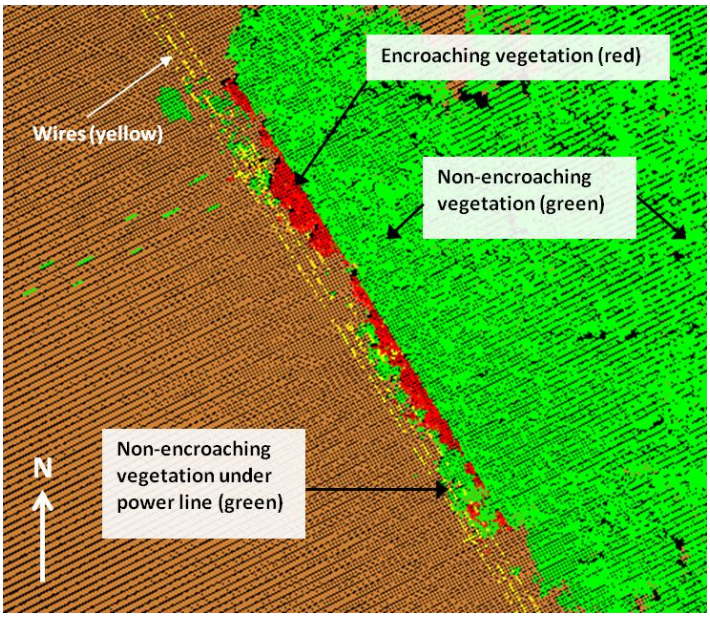

Figure16. *A sample of the results of the clear sky buffer operation in 2D space*

There is essentially now a separate class in LAS format that contains only vegetation encroachment LiDAR points. In this format, it is difficult to quantify how much encroaching vegetation must be dealt with in the field. The next series of steps were used to convert the 3D LiDAR vegetation encroachment data points to 2D polygons using GIS software. The main objective here was to enable the LiDAR vegetation encroachment points to represent regions where dangerous vegetation existed, rather than having 3D clusters of points. For many users, 2D data are easier to display, interpret, and quantify in order to make decisions, especially users with little or no experience in 3D GIS.

3.3. Encroaching Vegetation Polygons

LiDAR points in class 13, the vegetation encroachment class, were exported as ASCII text, and then converted to a point ESRI shape file. Since the text file contained X and Y coordinates along with elevation (Z) values for each point, the same data was transferred to the shape file upon conversion. The elevation of each encroachment point is known, but it would be more helpful for the user of the data to know how high above ground each point is as well. To derive the height above ground for each point, the elevation of the ground under each point must be subtracted from the Z value of the point. To do this the LiDAR ground points in class 2 were exported as a raster. The ground raster and vegetation encroachment point shape file were then brought into GIS software, where the ground elevation under each point was extracted and put in a new field called RASTERVALU (figure 17).

Extr_vals_to_ptsCopy

FID	Shape	X	Y	Z	CLASS	INTENSITY	RETURN	Count	RASTERVALU
382	Point ZM	406201.42	2251914.09	-43.82	13	120	1	1	-69.073456
383	Point ZM	406201.41	2251913.6	-43.65	13	33	1	1	-69.073456
384	Point ZM	406201.4	2251913.12	-43.41	13	56	1	1	-68.982285
385	Point ZM	406201.4	2251912.65	-42.95	13	84	1	1	-68.982285
386	Point ZM	406201.4	2251911.71	-41.6	13	70	1	1	-68.975128
387	Point ZM	406200.73	2251914.85	-44.32	13	135	1	1	-69.071144

Figure17. *The vegetation encroachment shape file with an additional field called RASTERVALU*

The new vegetation encroachment point shape file then contained all the original fields, plus a new field containing the ground elevation under each point. An additional attribute was then added, called HAGL, which would contain the height above ground of each encroachment point. A simple calculation of [Z] - [RASTERVALU] was made on the HAGL field to derive height above ground (figure 18).

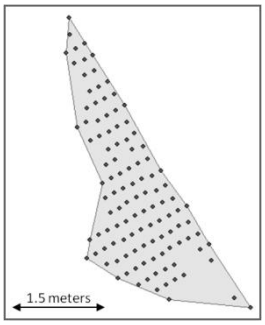

Figure18. *The vegetation encroachment shape file with an additional field called HAGL*

Next, the point shape file was converted to a polygon shape file using a point aggregation algorithm. The algorithm creates polygon features around clusters of proximate points. The aggregation distance was set to 1.5 meters, based on the general observed proximity of points to one another. The result was a series of polygons created from vegetation encroachment points within 1.5 meters of one another in 2D space (figure 19).

Extr_vals_to_ptsCopy

FID	Shape	X	Y	Z	CLASS	INTENSITY	RETURN	Count	RASTERVALU	HAGL
382	Point ZM	406201.42	2251914.09	-43.82	13	120	1	1	-69.073456	25.25345
383	Point ZM	406201.41	2251913.6	-43.65	13	33	1	1	-69.073456	25.42345
384	Point ZM	406201.4	2251913.12	-43.41	13	56	1	1	-68.982285	25.57228
385	Point ZM	406201.4	2251912.65	-42.95	13	84	1	1	-68.982285	26.03228
386	Point ZM	406201.4	2251911.71	-41.6	13	70	1	1	-68.975128	27.37512
387	Point ZM	406200.73	2251914.85	-44.32	13	135	1	1	-69.071144	24.75114

Figure19. *Encroachment polygon with associated points*

By default, the only meaningful attributes contained in the vegetation encroachment polygon shape file are Shape_ Leng, which shows the perimeter of each polygon, and Shape_ Area, which shows the area of each polygon. These attributes are helpful, but it would also be wise to take advantage of the precise and accurate elevation values associated with the point shape file the polygons were derived from. Additional statistics for the vegetation represented by each polygon would help a forestry contractor or utility company get a handle on the level of effort and cost associated with a vegetation removal project.

For this reason, statistics for heights (in the HAGL field) in the vegetation encroachment points that make up each polygon were imparted to every polygon through a spatial join. Three additional fields were added to the polygon shape file which will contain the mean, maximum, and minimum heights of points inside every polygon. These were called Mean_ HAGL, Max_ HAGL, and Min_ HAGL. Through the spatial join these fields were populated with their respective statistics. Another field was added by default, called Join_ Count, which shows the number of points that make up each polygon. The result was a series of vegetation encroachment polygons showing the number of points they are comprised of, and the mean, minimum and maximum heights of vegetation inside them (figure 20).

Table

Encroachment_Regions

FID	Shape *	Join_Count	Shape_Leng	Shape_Area	Min_HAGL	Max_HAGL	Mean_HAGL
10	Polygon ZM	139	69.965796	93.64047	20.215	85.227571	47.352336
11	Polygon ZM	14	16.917473	3.82106	29.850004	52.993998	49.774731
12	Polygon ZM	42	16.031744	11.825949	74.763505	82.671002	80.237322
13	Polygon ZM	3	8.625908	0.119427	33.6985	34.555666	34.102723
14	Polygon ZM	4	4.946257	0.076594	34.335996	34.665666	34.491582
15	Polygon ZM	7	13.968133	0.35536	34.101001	34.791001	34.325262
16	Polygon ZM	162	89.520776	162.320252	20.225797	36.861893	24.660082
17	Polygon ZM	496	234.709429	507.746578	24.896753	81.600288	53.741939
18	Polygon ZM	3	2.193873	0.17462	67.476337	68.143588	67.714504
19	Polygon ZM	61	29.389661	33.939419	28.728728	85.168498	71.959815
20	Polygon ZM	1256	131.744203	475.885588	31.323003	95.815505	88.234369

0 (0 out of 456 Selected)

Encroachment_Regions

Figure20. *Attributes of the final vegetation encroachment polygons*

4. RESULTS

In order to make the resulting data usable in a variety of applications, they were processed to include a shape file and KML version of the vegetation encroachment points, vegetation encroachment polygons, and power line conductor vectors. The points and polygons were already in shape file format, so they were then converted to KML. The conductor vectors were also exported as a shape file and then converted to KML. There are now points, polygons and lines in two exploitable formats (.shp and .kml) showing vegetation encroachment information and the conductors they threaten in the same two formats These data are actionable for vegetation removal efforts because they include coordinate, dimension, and height information.

The vegetation encroachment polygons were first viewed on top of the aerial image orthomosaic collected at the same time as the LiDAR data, in order to visually validate that encroachments exist where polygons indicate such a situation (figures 21, 22, and 23).

Figure21. *Vegetation inside a polygon obstructs the power line.*

Figure22. *Vegetation inside a polygon obstructs the power line.*

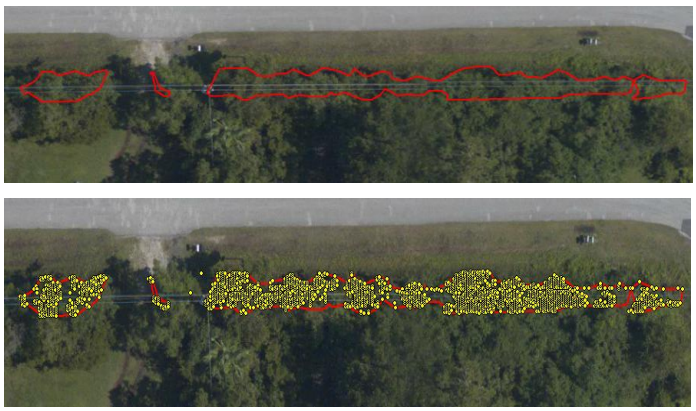

Figure23. *Vegetation inside several polygons is within 1.5 meters of the bottoms of the conductors – associated points displayed with polygons on the bottom.*

There are a variety of applications that can display and exploit the two formats of data produced in the previous section. This means the end user of the data need not purchase expensive software in order to fully take advantage of all the data has to offer. Of particular value are the attributes added to the vegetation encroachment polygons, which provide queues as to how much vegetation must be removed from a particular location and how tall the vegetation is. Figure 24 shows the vegetation encroachment polygons displayed in Arc Map labeled by the Shape_Area field. The polygons were categorized by area using a three class natural breaks classification, where green shows the group of smallest polygons, yellow the medium group, and red the group of largest polygons. The class groupings were 0.1 - 35 m^2, 35.1 – 137 m^2, and 137.1 – 475.4 m^2 respectively. The polygons could be labeled with any of the other attributes such as Min_AGL, Max_AGL, or Mean_AGL.

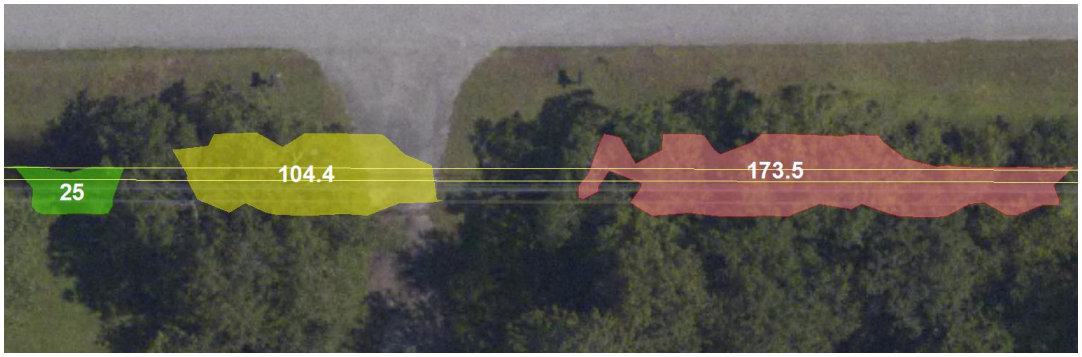

Figure24. *Vegetation encroachment polygons symbolized and labeled according to their areas in meters*

With the polygons labeled and symbolized by either area or one of the vegetation height attributes, planners of vegetation removal efforts can get a quick handle on what level of effort and cost would be associated with a particular project.

The same data in KML format can also be displayed in Google Earth, which anyone with an internet connection can obtain for free. In addition, the data user can view vector data over the seamless image orthomosaic provided by Google in the event no imagery was captured during a LiDAR mission (figure 25). Further, the Street View feature of Google Earth provides a unique way to visualize data. For instance, users of the data planning a vegetation removal effort can view encroachment and conductor data from the perspective of someone standing on the ground (figure 26). This is particularly useful for determining the feasibility of using specific equipment to remove vegetation, as the terrain or other obstructions could hinder removal efforts. The user has good situational awareness of removal sites without a visit to the field.

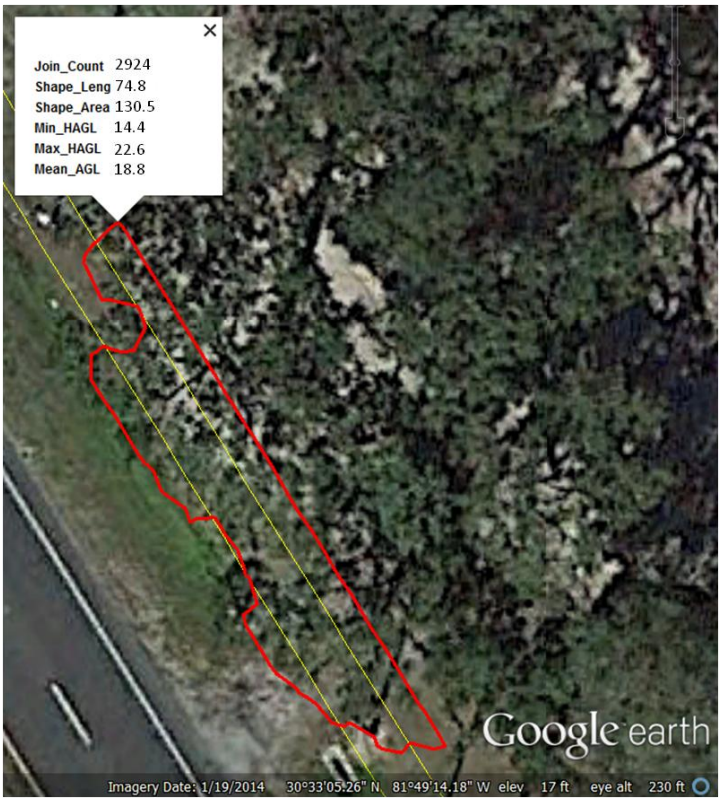

Figure25. *A vegetation encroachment polygon displayed in Google Earth with HTML popup showing attributes*

Figure26. *A vegetation encroachment polygon displayed in Google Earth in Street View mode*

In addition to the display of the vector data over imagery, general statistics about the vegetation encroachments in the study area were generated (table 3). A forestry contractor could potentially use these statistics to apply to a factor or a special formula determined to account for labor, equipment, and supply costs. Without LiDAR data, these statistics would be more difficult to generate.

Table3. *Statistics generated for the vegetation encroachment data.*

Polygon count	456
Maximum join count	5.134
Minimum join count	3
Mean join count	210
Total join count	95, 687
Minimum polygon length	0.1 m
Maximum polygon length	101.5 m
Mean polygon length	11.9 m
Total polygon length	5413.6 m
Maximum polygon area	144.9 m^2
Minimum polygon area	0.1 m^2
Mean polygon area	7 m^2
Total polygon area	3173.3 m^2
Average mean height above ground (all polygons)	10.8 m
Minimum height above ground (all polygons)	8.5 m
Maximum height above ground (all polygons)	12.9 m

5. DISCUSSION

LiDAR technology was employed in an effective way by using it to accurately identify vegetation with in a hazardous proximity to power distribution lines in the study area. The process started with a point cloud in LAS format and ended with vegetation encroachment polygons and conductor lines. The horizontal and vertical accuracies of the source LiDAR data were reported by the data vendor at <15 cm. This accuracy transfers to the vegetation encroachment polygons because no interpolation was performed. In other words, the envelopes of clusters (aggregations) of points became the polygons. For this reason, the polygons have a horizontal accuracy very close to the source LiDAR data sample point aggregations they were derived from. The final polygons are two-dimensional, so vertical accuracy is not applicable. However, the vegetation height statistics attribute values are taken directly from the elevation values of the source LiDAR data, so they take on the same vertical accuracy of <15 cm. The major drawback of using two-dimensional data is that it is not easy to get a good idea of the *volume* of vegetation that needs to be removed simply by looking at the data in a GIS or in map form. This is why the effort was made to at least include statistics about the vegetation heights within each polygon provided by the three-dimensional quality of the LiDAR data. The 2D data, however, can be used by a contractor to easily identify areas of vegetation where removal efforts should be focused in the field. Another drawback to this study was the fact that vegetation in the study area had already been trimmed away from the power lines before the analysis could be conducted. This prevented a ground truth validation of the vegetation encroachment polygons in the field.

The value of the type of vegetation encroachment data produced in this study is twofold. First, GIS-centric analysis of vegetation encroachments empowers decision makers in utility and forestry companies. They can put together a well-informed plan of action and budget to remove undesired vegetation based on knowing exactly where the vegetation is, accurately estimating how much there is, and prioritizing areas to be visited in the field. This can all be done in the office, with no visit to the field necessary. Second, the same data used to devise a vegetation removal plan and budget in the office can be used to locate candidate vegetation to be removed in the field. For instance, mobile phones, handheld devices such as tablets, and laptop computers can be used with the data in the field to locate removal sites through GPS tracking.

The key to the methodology used in this study was the ability to manipulate and process data with regard to spatial relationships (aggregation of points into polygons, spatial join, buffering, etc.), a fundamental capability of any GIS. The power of GIS was exercised in an effort to encourage utility companies to adopt new, technology-driven approaches to their vegetation management. Too often, purely physical methods involving human observation miss precarious situations where vegetation is too close to power lines. The prime example of this, of course, was the fact that vegetation which contacted power lines that caused the largest blackout in North America were inspected by humans in a helicopter only months prior.

6. CONCLUSION

This study demonstrated a methodology consisting of series of GIS operations to successfully identify vegetation within five feet of power lines and conductors from LiDAR data. The methodology started with preprocessing LiDAR point cloud, and then identifying power poles, power lines, and conductors. Encroaching vegetation (within 1.5 meter or five feet of power lines and/or conductors) was identified by utilizing 3D clear sky buffer, and then was converted to polygons in ESRI shapefile format and KML format for easy distribution. Compared to field survey, this method can save tremendous amount of labor and money, yet with high accuracy.

REFERENCES

Chen, G., Cheng, Z. F., Shi, K. Q., Zhang, J.,& Long, W., 2006.The application of LIDAR in surveying and design of power line. *Electric Power Survey & Design*, *5*, 012.

Edison Electric Institute, 2013.*The history of electricity* [online] Available at: <http://www.eei.org/ Pages/default.aspx> [Accessed 8 June 2013].

Ituen, I., Sohn, G., and Jenkins, A., 2008. A case study: Workflow analysis of power line systems for risk management. In: *The International Archives of the Photogrammetry, Remote Sensing and Spatial Information Sciences*, Volume XXXVII, Part B3b, Beijing, China, 3-11 July 2008.

Jobes,T., Moore, L., and Rousselle, A, 2008. Cutting-edge LiDAR exposes clearances. *Transmission and Distribution World*, May 2008, 40-46.

Mills, S., Gerrardo, M., Li, Z., Cai, J., Hayward, R.F., Mejias, L, and Walker, R.A., 2010.Evaluation of aerial remote sensing techniques for vegetation management in power line corridors [pdf]. *IEEE Transactions on Geosciences and Remote Sensing*, 48(9),3379-3390.

Narolski, S., 2010.Is that tree too close? *Transmission and Distribution World*, July 2010, 46-51 [online]. Available at: <http://tdworld.com/%5Bprimary-term%5D/tree-too-close> [Accessed 10 June 2013].

Texas Engineering Experiment Station, 2011.*Best practices in vegetation management for enhancing electric service in texas.* College Station: Texas Engineering Experiment Station.

U.S.-Canada Power System Outage Task Force, 2004.*Final report on the august 14, 2003 blackout in the united states and canada: causes and recommendations.* United States and Canada: U.S.-Canada Power System Outage Task Force.

Yang, F. and Xu, Z. J.,2009. Application of the LiDAR technology on operation and maintenance of power transmission Lines. *Southern Power System Technology*,2, 023.

You, A.,Han, X., Wang, X., & Tang, D., 2013.Applications of LiDAR in patrolling electric-power lines. In *Technological Advances in Electrical, Electronics and Computer Engineering (TAEECE), 2013 International Conference* (pp. 110-114).

Young, J., 2011. *LiDAR for dummies.* [pdf] Hoboken: Wiley. Available at: <http:// www.dlt.com/ library/ whitepaper/lidar-for-dummies-ebook> [Accessed 7 July 2013].

Zhang, X. F., Chen, G., Long, W., Cheng, Z. F., & Zhang, K., 2008. Current status and prospects of helicopter power line inspection tour with LiDAR. *Electric Power Construction*,3, 013.

AUTHORS' BIOGRAPHY

Brian Kurinsky graduated from Northwest Missouri State University with a MS in GI Science in 2014. He currently is working in the private industry on LiDAR related projects.

Ming-Chih Hung is an Associate Professor of Geography in Northwest Missouri State University. His research interests are remote sensing and GIS on urban studies as well as environmental issues.